# Maximum-Entropy Method in the analysis of Charge Density I

- *A Promising Tool for Charge Density Study* -

Masaki Takata
RIKEN SPring-8 Center

# Outline

1. Information Entropy and Charge Density Analysis
2. MEM Charge Density Study by Diffraction Data
3. Charge Density Refinement by MEM

   MEM/Rietveld Analysis etc.
4. Nuclear Density Study by MEM
5. Application

## Information Theory (1948)

***I just wondered how things were put together.***

*by Claude Shannon*

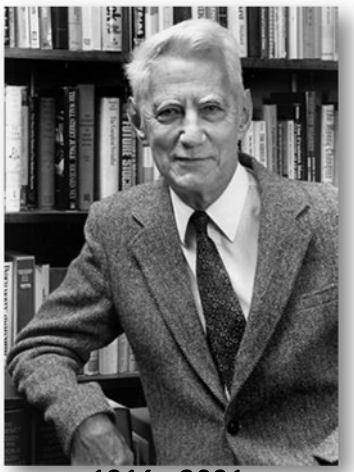

1916 - 2001

American mathematician and electronic engineer known as "the father of information theory"

**Information Entropy :**

$$S = -\sum_i \rho_i \, \ell n \rho_i$$

as a measure for the uncertainty of information (data)

DEDICATED TO: EDWIN THOMPSON JAYNES

*July 5, 1922 to April 30, 1998*

**Jaynes' Entropy (1968)**

$$S = -\sum_i \rho_i \, \ell n \frac{\rho_i}{\tau_i}$$

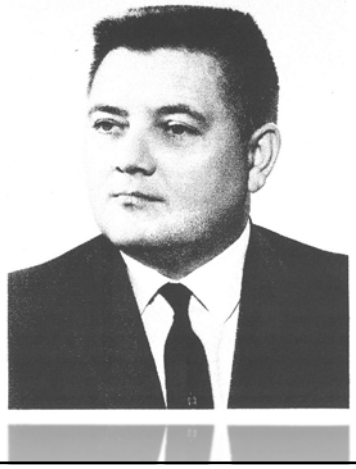

**Innovation of the idea:**

**Prior information** $\tau$

## Application to Image Reconstruction Maximum Entropy Method

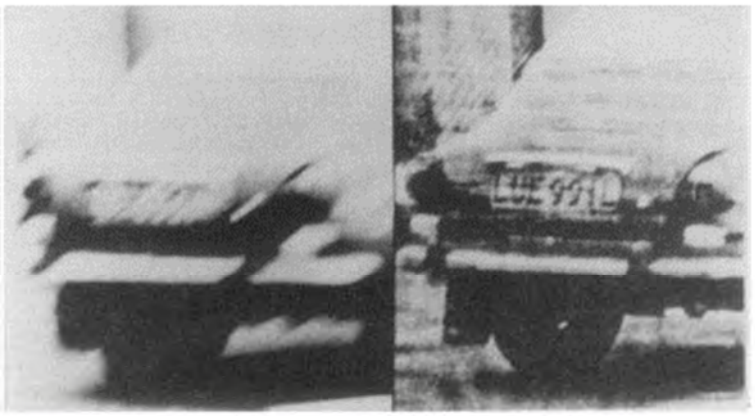

Data Reconstruction

Silver, R.N.,Sivia,D.S. and Gull,J.E.:*Phys.Rev.*B41 2380-2389(1990)

***The Dawn of MaxEnt Application to Charge Density Study***

*Nature Vol. 298 1 July 1982*

**Electron density images from imperfect data by iterative entropy maximization**

**Douglas M. Collins**
Department of Chemistry, Texas A & M University, College Station, Texas 77843, USA

**Information theory provides a uniquely powerful apparatus for reconstructing an image from imperfect data in its dual space. An iterative procedure based on constrained entropy maximization is presented here for reconstruction of electron density from imperfect single-crystal X-ray diffraction data. In the ideal situation, continuous electron density, its periodicity given by the lattice, is the Fourier transform of an infinite set of structure factors whose squared moduli are observables. An ideal electron density is unattainable from experiment because of the common experimental inadequacies of incomplete and noisy data discussed by Gull and Daniell[1]. These inadequacies are partially overcome in the present procedure which yields true super-resolution and is economical even for protein crystal structures as illustrated.**

**Although Gull and Daniell[1] focused on radioastronomical**


*Acta Cryst.* (1993). D**49**, 37-60

**Direct Phase Determination by Entropy Maximization and Likelihood Ranking: Status Report and Perspectives**

BY G. BRICOGNE
*MRC Laboratory of Molecular Biology, Hills Road, Cambridge CB2 2QH, England, and LURE, Bâtiment 209D, Université Paris-Sud, 91405 Orsay, France*

*(Received 29 June 1992; accepted 15 October 1992)*

**Abstract**

A new multisolution phasing method based on entropy maximization and likelihood ranking, proposed for the specific purpose of extending probabilistic direct methods to the field of macromolecules, has been implemented in two different computer programs and applied to a wide variety of problems. The latter comprise the determination of small crystal structures from X-ray diffraction data obtained from single crystals or from powders, and from electron diffraction data partially phased by image processing of electron micrographs; the *ab initio* generation and ranking of phase sets for small proteins; and the improvement of poor quality phases for a larger protein at medium resolution under constraint of solvent flatness. These applications show that the primary goal of this new method – namely increasing the accuracy and sensitivity of probabilistic phase indications compared with conventional direct methods – has been achieved. The

**0. Introduction**

The *ab initio* determination of macromole
by a purely computational solution to th
used to be the secret dream of most pro
phers beginning their careers. A whole de
ockological frenzy may however have distracted the attention


*Acta Cryst.* (1993). A**38**, 47-60

**Statistical Geometry. I. A Self-Consistent Approach to the Crystallographic Inversion Problem Based on Information Theory**

BY STEPHEN W. WILKINS*
*CSIRO, Division of Chemical Physics, PO Box 160, Clayton, Victoria, Australia 3168 and Institut Laue-Langevin, BP156 Centre de Tri, Grenoble Cedex 38042 France*
JOSEPH N. VARGHESE
*CSIRO, Division of Protein Chemistry, Royal Parade, Parkville, Victoria, Australia 3052*
AND MOGENS S. LEHMANN
*Institut Laue-Langevin, BP156 Centre de Tri, Grenoble Cedex 38042 France*

*(Received 11 October 1983; accepted 1 July 1982)*

**Abstract**

The problem of inverting crystallographic diffraction data to obtain structural information is examined within the maximum-entropy formulation of information theory. The principal features of the present method (normal statistical geometry) are: (i) all predictions of the method are consistent with the given information (constraints) and least biased with respect to missing information; (ii) the adoption of weak (typically non-linear) constraints for incorporating the major part of the structural information guarantees that a solution exists in practice and leads to filtering of the structure maps consistent with the accuracy of the data; (iii) general conditions are established which lead to unique solutions for the structure map; (iv) atomicity is not a prerequisite; (v) other methods of crystallographic inversion may be incorporated via the adoption of appropriate constraint relations; and (vi) the task of numerical solution is roughly linear in the

## *MEM application to crystallography*

***Electrostatic Potential Imaging***

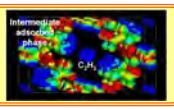

**MEM: Virtual Lens for *Diffraction Data Imaging***

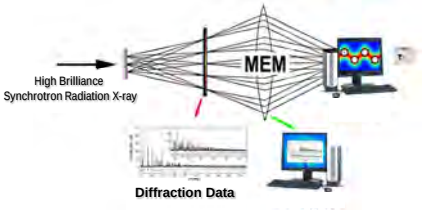


**Structure Model Refinement**

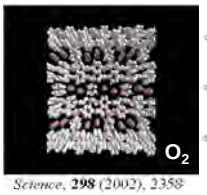


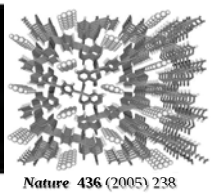

*Science*, **298** (2002), 2358 *Nature* **436** (2005) 238

Gas Molecule Imaging Adsorbed in MOF

**Bonding Nature Visualization**

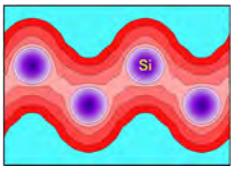


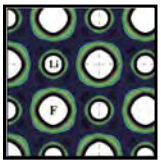


Covalent Bonding Ionic Bonding

**Charge Order Imaging**

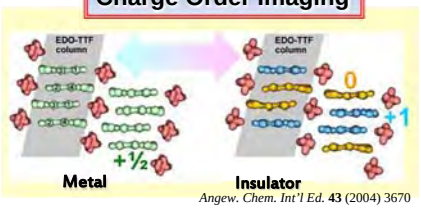


*Angew. Chem. Int'l Ed.* **43** (2004) 3670

*Charge Ordering Through M-I Transition of EDO-TTF*

## 2. MEM Charge Density by Diffraction Data

**From Electron Density mapping**

**To Electrostatic Potential visualizing**

**X-ray Scattering**

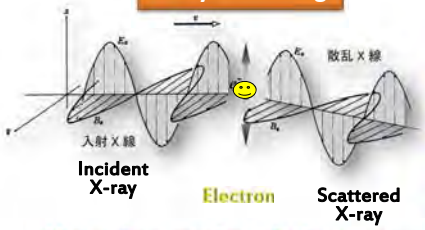


**X-ray is a probe of electron.**

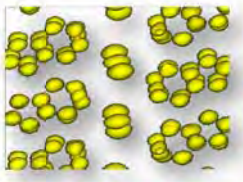

**ρ(r): Electron density in material**

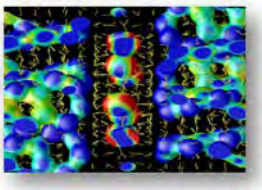

**Electrostatic Potential Imaging**

**To visualize precise charge density & electrostatic potential**

**1.Reliable Diffraction Data:** *absorption, extinction, etc. data correction free*

**2.Sophisticated Data Analysis Technique**

*Maximum Entropy Method(MEM), Multipole refinment, etc.*

## Basic Concept: MEM Analysis

The formalism of the constrained entropy is given by using the method of Lagrange undetermined multiplier in order to constrain the function C to be unity while maximizing the entropy.


**X-ray Data**

$$F_{cal}(k) = \sum_{r} \rho(r) \exp[2\pi i k r]$$

| h k l | $F_{obs}$ |
|---|---|
| 0 0 0 | 112.000 |
| 1 1 1 | -60.131(2) |
| 2 2 0 | -67.343(3) |
| 1 1 3 | -43.634(1) |
| 4 0 0 | -56.234(2) |
| ... | ... |
| 6 6 4 | 19.126(1) |

Extinction Free Precise Data by Pendellösung Method Saka & Kato, Acta Cryst. (1986)


$$Q(\lambda) = -\sum_{\mathbf{r}} \rho'(\mathbf{r}) \ell n \frac{\rho'(\mathbf{r})}{\tau'(\mathbf{r})} - \frac{\lambda}{2}(C-1)$$

$$C = \frac{1}{N} \sum_{\mathbf{k}} \frac{|F_{cal}(\mathbf{k}) - F_{obs}(\mathbf{k})|^2}{\sigma^2(\mathbf{k})}$$

**MEM**

To maximize the entropy by $\frac{\partial Q(\lambda)}{\partial \rho'(\mathbf{r})} = 0$

**Charge Density**

$$\rho(r) = \sum_{k} F(k) \exp[-2\pi i k r]$$

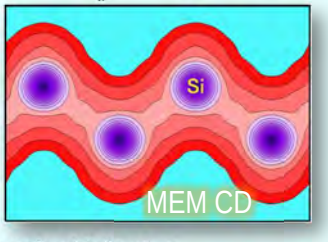


**MEM charge density formalism is obtained as**

$$\rho(\mathbf{r}) = exp\left[ \ell n\, \tau(\mathbf{r}) + \frac{\lambda F_0}{N} \sum_{\mathbf{k}} \frac{1}{\sigma^2(\mathbf{k})} \{F_{obs}(k) - F_{cal}(k)\} exp(-2\pi i \mathbf{k} \cdot \mathbf{r}) \right]$$

## The process of obtaining the MEM solution


Charge Distribution (110) Plane

Initial solution

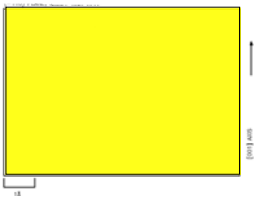

After 2nd iteration

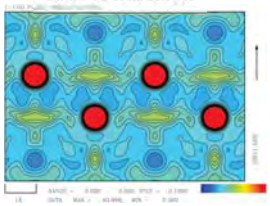

1D Charge Density <111> Direction

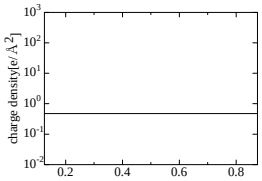


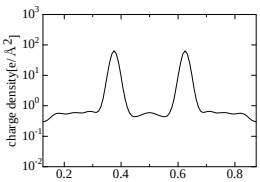


Coincidence of Atomic Scattering Factor

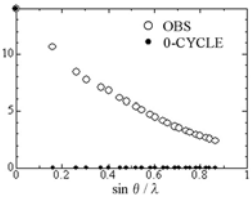


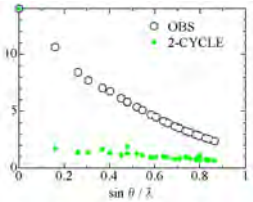

## The iterative process of obtaining the MEM solution

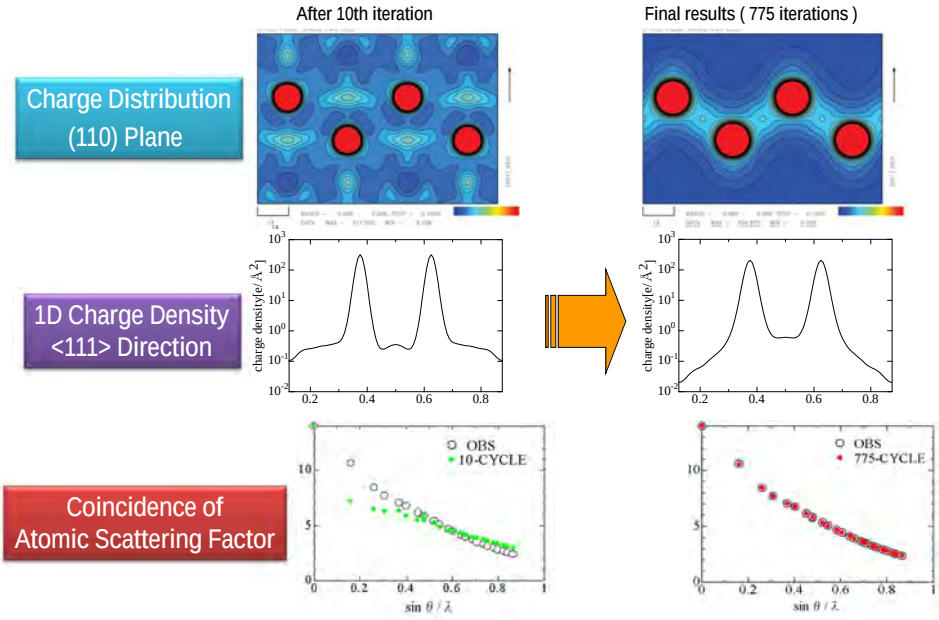


## The Sketch of Electron Density & Fourier Coefficient Distribution

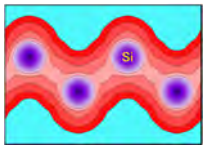


Covalent Bond Model

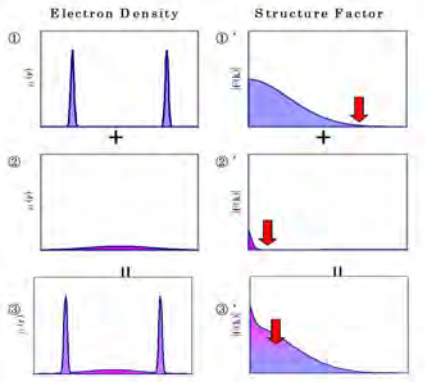


***Estimated Atomic Scattering Factors by MEM***

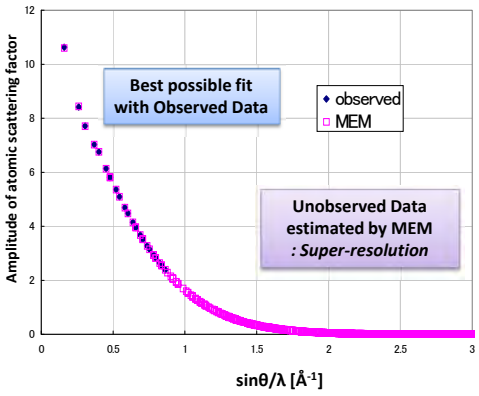

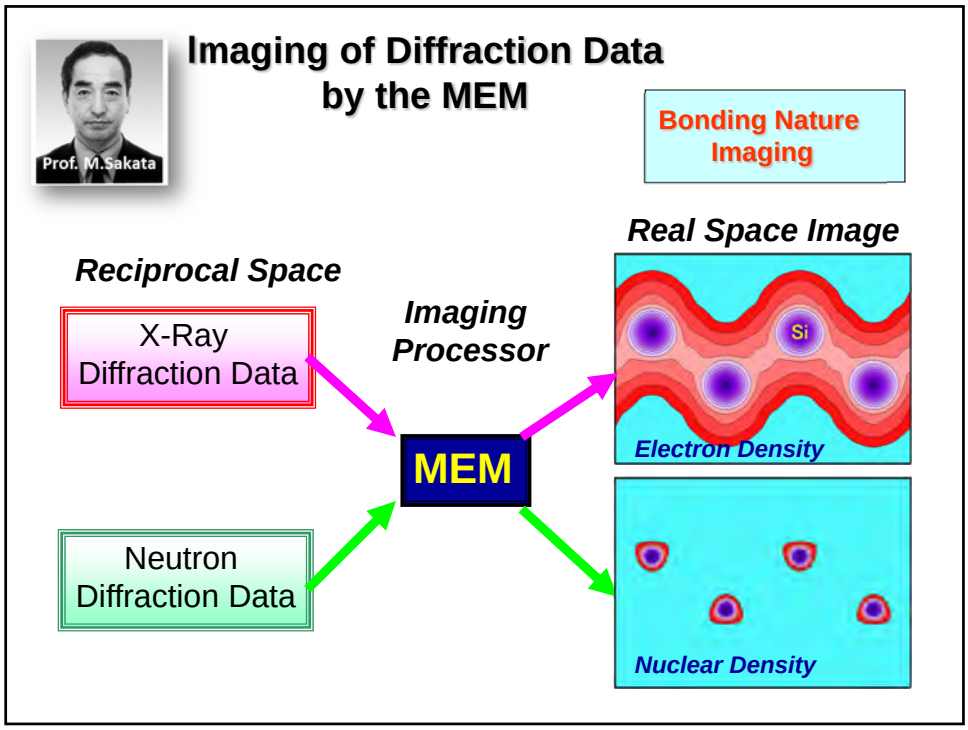
Prof. M.Sakata
Imaging of Diffraction Data by the MEM
Bonding Nature Imaging
Real Space Image
Reciprocal Space
X-Ray Diffraction Data
Imaging Processor
MEM
Neutron Diffraction Data
Si
Electron Density
Nuclear Density

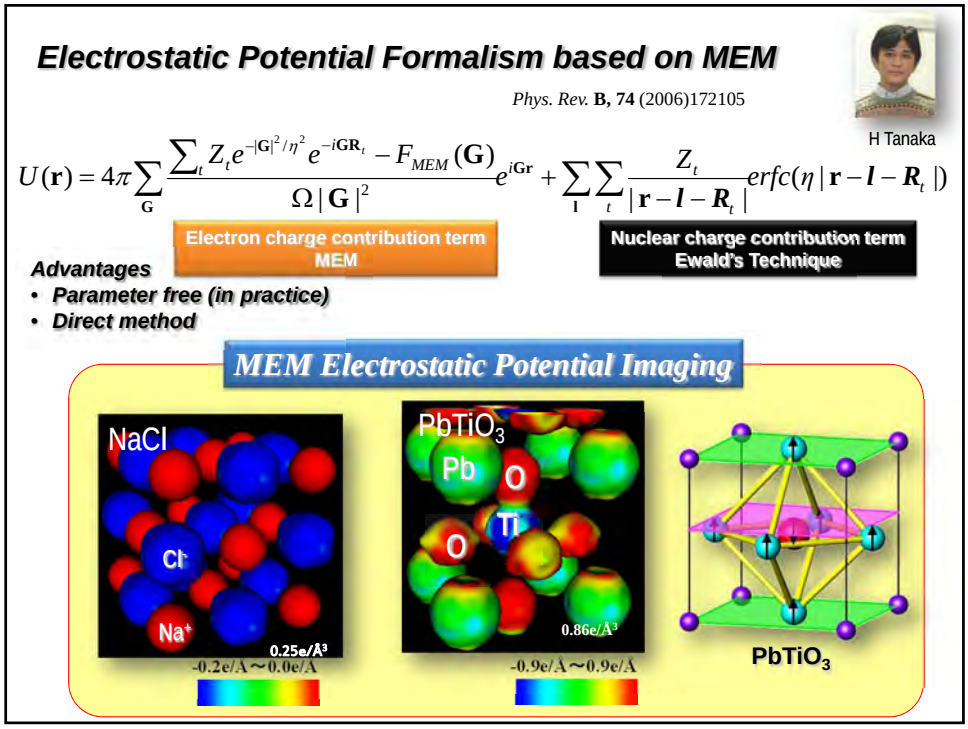
Electrostatic Potential Formalism based on MEM
Phys. Rev. B, 74 (2006)172105
H Tanaka
$U(\mathbf{r}) = 4\pi \sum_{\mathbf{G}} \frac{\sum_t Z_t e^{-|\mathbf{G}|^2/\eta^2} e^{-i\mathbf{G}\mathbf{R}_t} - F_{MEM}(\mathbf{G})}{\Omega |\mathbf{G}|^2} e^{i\mathbf{G}\mathbf{r}} + \sum_{\mathbf{l}} \sum_t \frac{Z_t}{|\mathbf{r}-\mathbf{l}-\mathbf{R}_t|} erfc(\eta |\mathbf{r}-\mathbf{l}-\mathbf{R}_t|)$
Electron charge contribution term MEM
Nuclear charge contribution term Ewald's Technique
Advantages
• Parameter free (in practice)
• Direct method
MEM Electrostatic Potential Imaging
NaCl
Cl
Na+
0.25e/Å3
-0.2e/Å~0.0e/Å
PbTiO3
Pb
O
Ti
O
0.86e/Å3
-0.9e/Å~0.9e/Å
PbTiO3

# MaxEnt Visualization of Charge Density Information in Materials

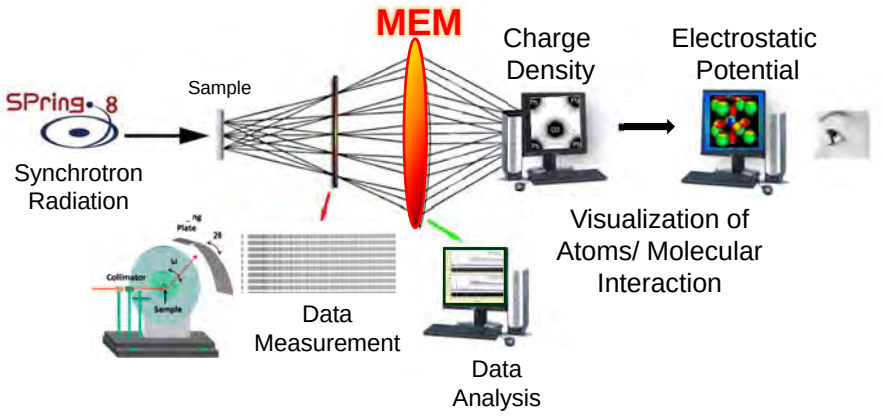


## Be Charge Density Study by Precise Single Crystal Data

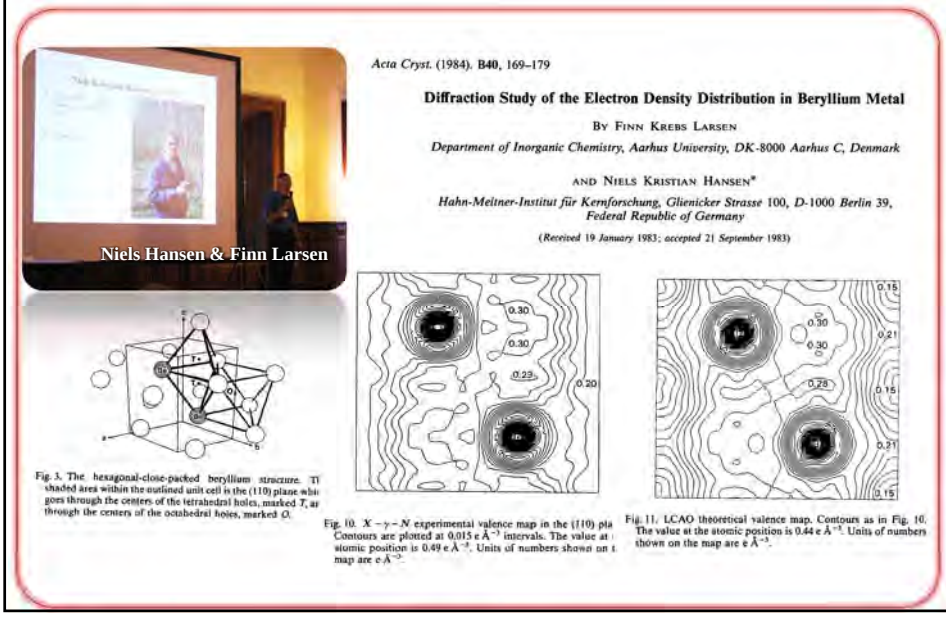

# MEM Charge Density Study of Be




*M.Takata, B.Iversen, F.Larsen, et al. Acta Cryst* (1994) **A50** 330

*Acta Cryst.* (1995). B51, 580–591

**Experimental Evidence for the Existence of Non-nuclear Maxima in the Electron-Density Distribution of Metallic Beryllium. A Comparative Study of the Maximum Entropy Method and the Multipole Refinement Method**


BY BO BRUMMERSTEDT IVERSEN AND FINN KRIBY LARSEN†

*Department of Chemistry, Aarhus University, DK 8000 Aarhus C, Denmark*

MOHAMMED SOUHASSOU‡

*Medical Foundation of Buffalo, Buffalo, NY 14214, USA*

AND MASAKI TAKATA

*Department of Applied Physics, Nagoya University, Nagoya 464-01, Japan*



(Received 9 May 1994; accepted 12 September 1994)


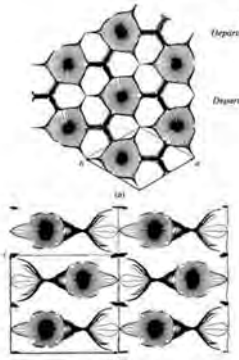



[110]

(b)

Fig. 2. Gradient paths of the electron-density distribution obtained with the MEM. (a) and (b) are the (001) and (110) planes, respectively.

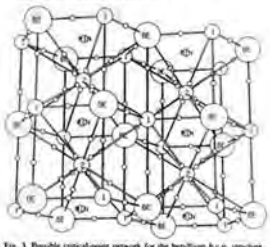

Fig. 3. Possible critical-point network for the beryllium h.c.p. structure obtained from the topological analysis of the MEM electron-density distribution. The non-nuclear maxima NNM1 and NNM2 are marked 1 and 2, respectively. The CAGE point is marked MIN.

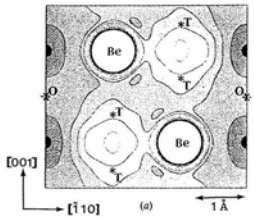


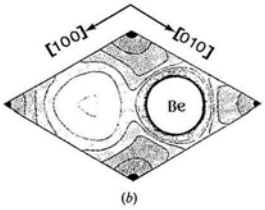


(b)

# Problem: The Influence of the Data Completeness Si MEM Charge Density by Takata & Sakata



*Acta Cryst.* (1996). **A52**, 287–290

**The Influence of the Completeness of the Data Set on the Charge Density Obtained with the Maximum-Entropy Method. A Re-examination of the Electron-Density Distribution in Si**


MASAKI TAKATA AND MAKOTO SAKATA

*Department of Applied Physics, Nagoya University, Nagoya 464-01, Japan*



(Received 17 July 1995; accepted 30 October 1995)



**Abstract**

The charge densities derived with the maximum-entropy method (MEM) may be influenced to some extent by the completeness of the data set. In order to examine the effects of the incompleteness, structure-factor data of Si measured by the *Pendellösung* method [Saka & Kato (1986). *Acta Cryst.* A**42**, 469–478] were re-analysed by the MEM. This data set is incomplete: it contains all space-group-allowed reflections with $\sin\theta/\lambda = 0.86$ Å$^{-1}$, and in addition 844 and 880 with $\sin\theta/\lambda = 1.04$ Å$^{-1}$. Results of a MEM analysis of the complete subset of data are compared with those from the full but incomplete set published previously [Sakata & Sato (1990). *Acta Cryst.* A**46**, 263–270]. The smaller but complete set was found to give a smooth charge-density distribution that is consistent with previous theoretical work. It is found that the sharp peak maximum at the bond midpoint reported previously is exaggerated owing to the highest-order reflection 880. The completeness of the data set appears to be one of the key factors for obtaining reliable charge densities with MEM. The incompleteness of the data set may cause non-physical fine features of the MEM density distribution.

Therefore, the reliability of the data is very important and will directly influence the results. Significant systematic errors in the observed data are expected to artificially deform the resultant MEM density. They will always tend to deteriorate the MEM map. Recently, Jauch (1994) has pointed out that MEM maps are susceptible to exhibiting similar artifacts to those inherent in Fourier inversion depending on data completeness, error accumulation at special positions *etc*. Consequently, it is very important to reduce all kinds of systematic errors as much as possible in order to construct an 'accurate' electron density from observed data with the MEM. Recently, it has been claimed that non-physical fine features found in the MEM density are probably due to the non-uniform residual distributions of $\chi^2$ (Jauch & Palmer, 1993). From the simulation using the model charge density of a hypothetical crystal, De Vries, Briels & Feil (1994) have proposed a weighting scheme that leads to more uniform residual distributions and gives a smoother density. It is plausible that many factors may influence the MEM charge densities. It is necessary to study all these factors as much as possible before reaching a full understanding of the meaning of the MEM charge densities. In this paper, the influence of the


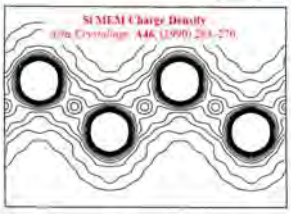


Fig. 1. The (110) MEM charge density of Si based on the full set of data measured by Saka & Kato. The contour lines are drawn from 0.0 to 2.0 e Å$^{-3}$ with a step of 0.1 e Å$^{-3}$.

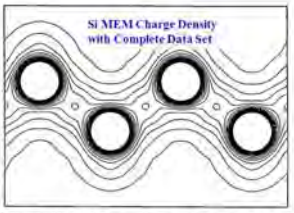


Fig. 2. The (110) MEM charge density of Si based on the data set complete out to 664. The contour lines are drawn from 0.0 to 2.0 e Å$^{-3}$ with a step of 0.1 e Å$^{-3}$.

## Data Incompleteness gave an artifact in MEM density.

endellösung Method Data
Saka & Kato
Acta Cryst. (1986)

Table 1. *Observed, $F_{obs}$, and calculated, $F_{MEM}$, structure factors for the MEM results based on the incomplete and complete data sets*

| | | | Incomplete set | | Complete set | |
|---|---|---|---|---|---|---|
| *h* | *k* | *l* | $F_{obs}$ | $F_{MEM}$ | $F_{obs}$ | $F_{MEM}$ |
| 1 | 1 | 1 | 60.13 (5) | 59.97 | 60.13 (5) | 59.98 |
| 2 | 2 | 0 | 67.34 (5) | 67.52 | 67.34 (5) | 67.52 |
| 3 | 1 | 1 | 43.63 (3) | 43.61 | 43.63 (3) | 43.61 |
| 4 | 0 | 0 | 56.23 (4) | 56.22 | 56.23 (4) | 56.22 |
| 3 | 3 | 1 | 38.22 (3) | 38.23 | 28.22 (3) | 38.23 |
| 4 | 2 | 2 | 49.11 (3) | 49.06 | 49.11 (3) | 49.06 |
| 5 | 1 | 1 | 32.94 (2) | 32.95 | 32.94 (2) | 32.95 |
| 3 | 3 | 3 | 32.83 (2) | 32.84 | 32.83 (2) | 32.84 |
| 4 | 4 | 0 | 42.88 (3) | 42.88 | 42.88 (3) | 42.88 |
| 5 | 3 | 1 | 28.81 (2) | 28.82 | 28.81 (2) | 28.82 |
| 6 | 2 | 0 | 37.59 (6) | 37.53 | 37.59 (6) | 37.53 |
| 5 | 3 | 3 | 25.36 (4) | 25.35 | 25.36 (4) | 25.35 |
| 4 | 4 | 4 | 33.18 (5) | 33.19 | 33.18 (5) | 33.18 |
| 7 | 1 | 1 | 22.37 (3) | 22.37 | 22.37 (3) | 22.37 |
| 5 | 5 | 1 | 22.42 (3) | 22.41 | 22.42 (3) | 22.41 |
| 6 | 4 | 2 | 29.42 (4) | 29.43 | 29.42 (4) | 29.44 |
| 5 | 5 | 3 | 19.98 (3) | 19.97 | 19.98 (3) | 19.97 |
| 7 | 3 | 1 | 19.90 (3) | 19.90 | 19.90 (3) | 19.91 |
| 8 | 0 | 0 | 26.23 (4) | 26.23 | 26.23 (4) | 26.23 |
| 7 | 3 | 3 | 17.83 (3) | 17.83 | 17.83 (3) | 17.83 |
| 8 | 2 | 2 | 23.48 (4) | 23.49 | 23.48 (4) | 23.49 |
| 6 | 6 | 0 | 23.48 (4) | 23.49 | 23.48 (4) | 23.49 |
| 7 | 5 | 1 | 15.98 (2) | 15.98 | 15.98 (2) | 15.98 |
| 5 | 5 | 5 | 15.98 (2) | 15.98 | 15.98 (2) | 15.98 |
| 8 | 4 | 0 | 21.15 (3) | 21.15 | 21.15 (3) | 21.15 |
| 9 | 1 | 1 | 14.46 (2) | 14.46 | 14.46 (2) | 14.46 |
| 7 | 5 | 3 | 14.43 (2) | 14.43 | 14.43 (2) | 14.43 |
| 6 | 6 | 4 | 19.13 (3) | 19.13 | 19.13 (3) | 19.13 |
| 9 | 3 | 1 | | 12.97 | | 12.93 |
| 8 | 4 | 4 | 17.44 (3) | 17.44 | | 17.22 |
| 7 | 7 | 1 | | 11.91 | | 11.67 |
| 9 | 3 | 3 | | 11.78 | | 11.68 |
| 7 | 5 | 5 | | 11.86 | | 11.75 |
| 10 | 2 | 0 | | 15.65 | | 15.59 |
| 8 | 6 | 2 | | 15.75 | | 15.55 |
| 9 | 5 | 1 | | 10.70 | | 10.59 |
| 7 | 7 | 3 | | 10.75 | | 10.61 |
| 9 | 5 | 3 | | 9.80 | | 9.61 |
| 10 | 4 | 2 | | 12.95 | | 12.77 |
| 7 | 7 | 5 | | 8.82 | | 8.75 |
| 8 | 8 | 0 | 12.41 (2) | 12.41 | | 11.61 |

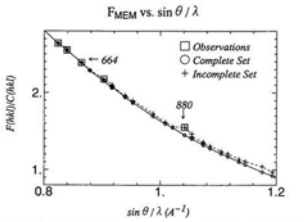


Fig. 3. The observed and calculated values of $F(hkl)/C(hkl)$ against $\sin\theta/\lambda$. $C(hkl)$ is the trigonometric factor [$C = 8$ (even order), $4 \times 2^{1/2}$ (odd order)].

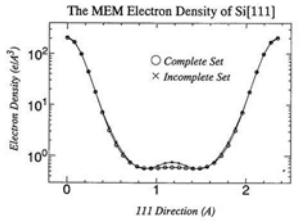


Fig. 4. The one-dimensional charge densities of Figs. 1 and 2 are plotted on a logarithmic scale along the bonding direction between the atoms.

## A way for reliable data measurement for MEM analysis
- SR Large Debye-Scherrer Camera -

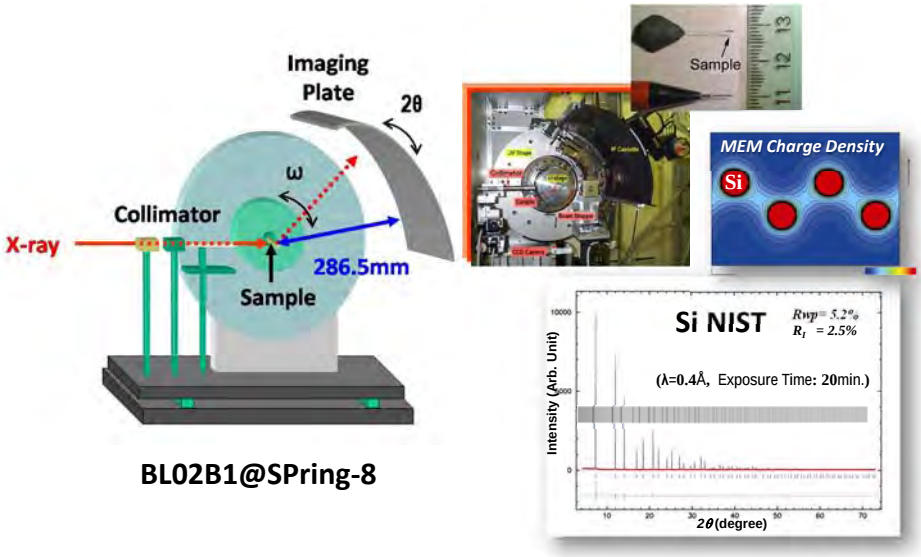


**BL02B1@SPring-8**

## Si(NIST) Powder Diffraction Data

complete data set with no absorption correction
(λ=0.4Å, exposure time: 20min.)

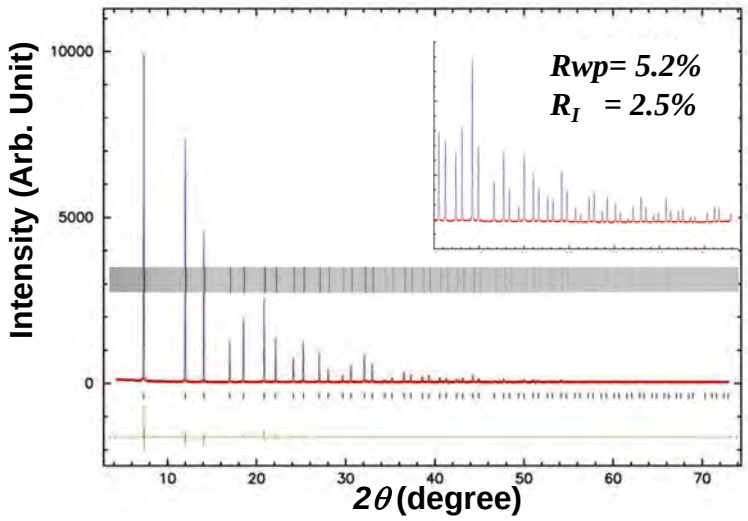


## Si & Diamond MEM Charge Densities Based on SR Powder Diffraction Data

*(100K)*

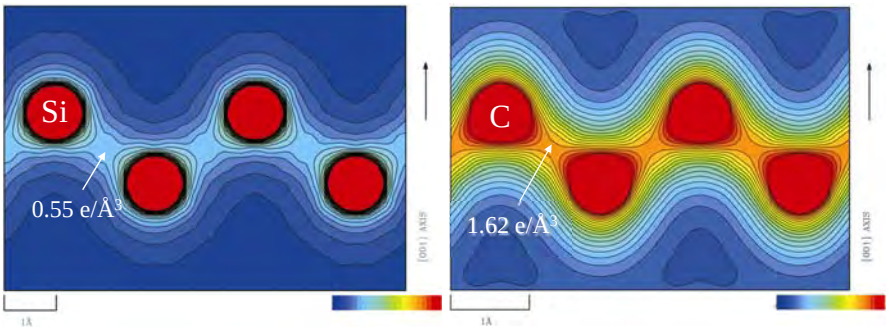


0.0～2.0 0.1[e/Å$^3$]step

## Comparison with Theoretical Charge Density

*Reliable data can give a meaningful precise charge density by MEM.*

Si Valence Electron Density

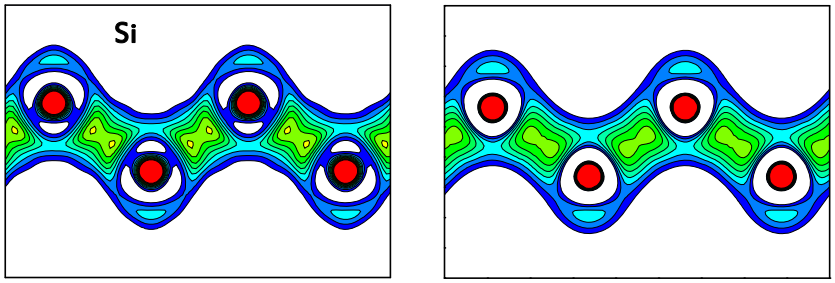


MEM Charge Density

First Principle Calculation
Wien 2000

## The IP Camera Powder Method using High Energy SR

- **Whole Powder Pattern can be collected simultaneously.**

  *Rapid data collection*
  *No need of incident X-ray beam monitoring*
  *Same experimental conditions at each data point*

- **High Resolution Data**

  *$\lambda$=0.5Å~1.0Å  d= 0.4Å~0.8Å at 80º (2$\theta$)*

- **Insignificant 2$\theta$ dependence of absorption effects even for heavy materials**

  *For example  $PbTiO_3$ powder in 0.1$\phi$ capillary*

| X-ray Energy | $\mu$ ($mm^{-1}$) | $\mu_{0^\circ}$ / $\mu_{90^\circ}$ (%) |
|---|---|---|
| MoK$\alpha$(0.71Å) | 68.2 | 24.0 |
| 30KeV(0.41Å) | 17.2 | 1.7 |

**$\mu$ : Total linear absorption coefficient**
**$\mu_{0^\circ}$ / $\mu_{90^\circ}$ : The ratio of the coefficient at 0º and 90º(2$\theta$)**

# $PbTiO_3$ MEM Charge Densities based on high energy powder data

Prof. Y.Kuroiwa

λ=0.41Å : 30keV, Exposure Time : 60 min., *d* >0.47Å

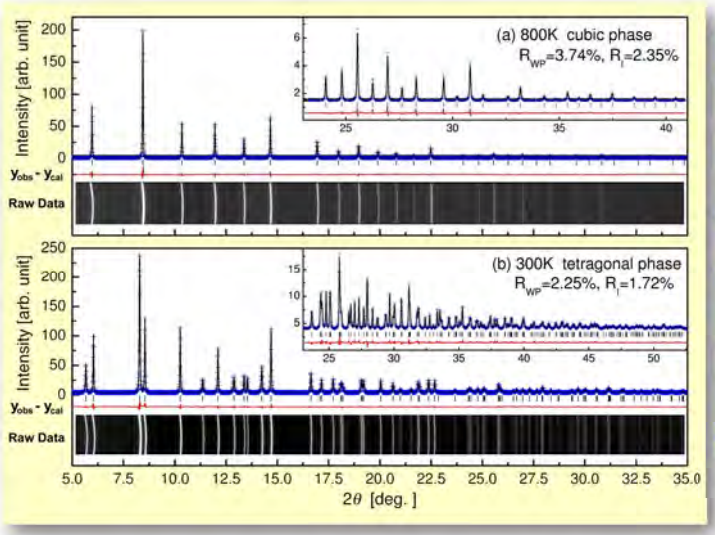


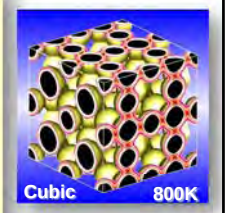


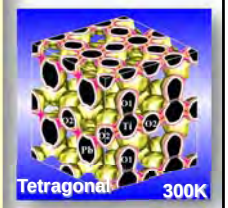


*Y. Kuroiwa et al., Phys. Rev. Lett. 87 (2001) 217601*

## A way to estimate net charge of atoms

**Extended Mulliken Scheme for MEM CD Analysis**

**Net charge of *A* atom**

$$-\Delta Q_A = \sum_{i \in A} Q_i - Z_A$$

$Z_A$: Atomic Number

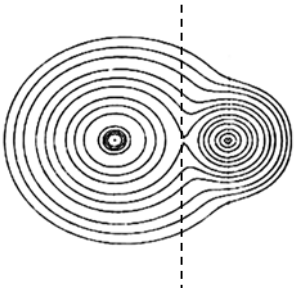

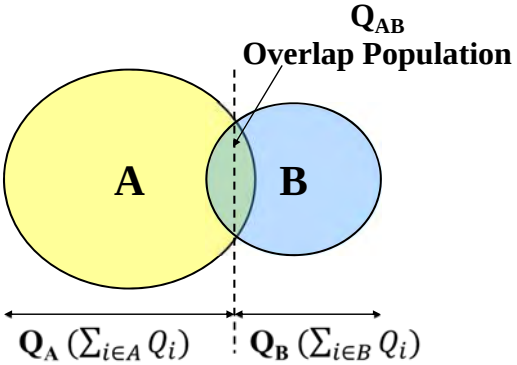


**Orbital Population**

## Ionic Valence investigation from MEM charge Density

| | $BaTiO_3$ | | $PbTiO_3$ | | $PbZrO_3$ |
|---|---|---|---|---|---|
| | tetragonal | cubic | tetragonal | cubic | cubic |
| A: Pb, Ba | +1.9(3) | +1.8(3) | +1.1(3) | +2.0(3) | +1.2(4) |
| B: Ti, Zr | +1.9(4) | +2.1(4) | +2.4(4) | +2.2(3) | +2.7(5) |
| O (1) | -1.6(3) | -1.3(3) | -1.4(3) | -1.4(3) | -1.3(2) |
| O (2) | -1.1(3) | - | -1.0(3) | - | - |

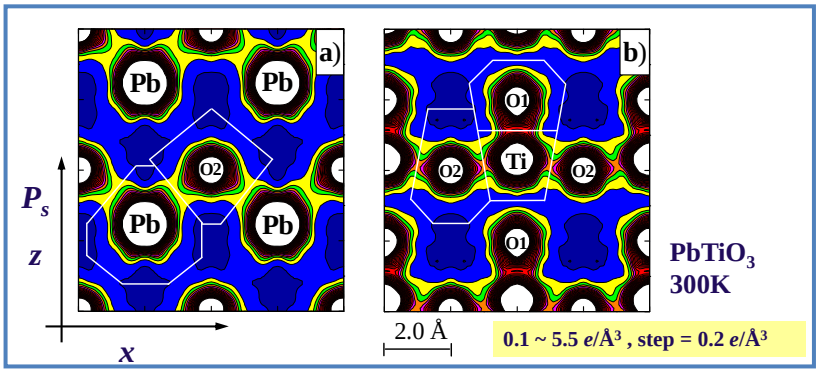


## High counting statistics data measurement for MEM Overlaid Measurement Method

Prof. E.Nishibori

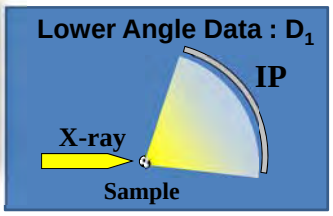


+

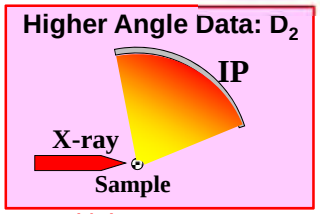


*With longer exposure*

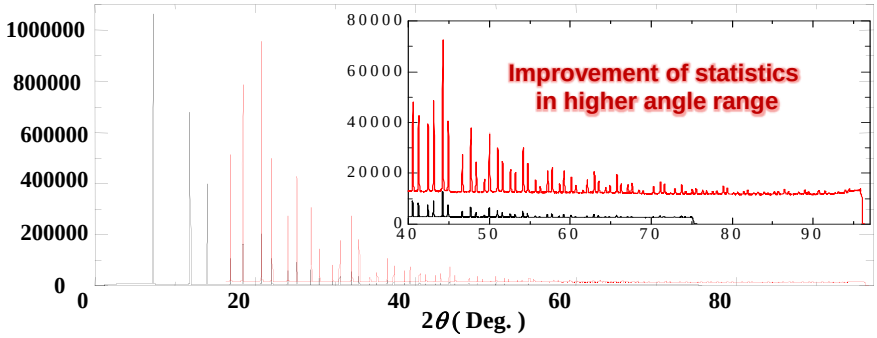

## MEM valence density by overlaid measurement

**With d > 0.34 Å**

E. Nishibori *et al.*,
Acta. Cryst. A (2007)

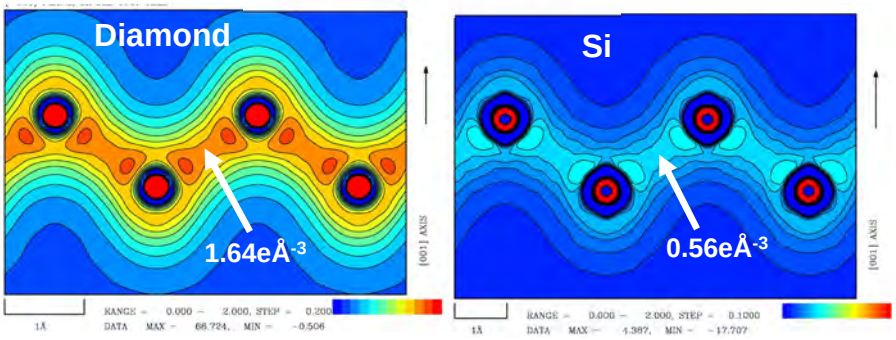


**Diamond: 1.53∼1.69eÅ$^{-3}$** **Si: 0.55∼0.59eÅ$^{-3}$**

Theoretical charge density values at the bond midpoint

Yin M. T. And Cohen M. L., PRB26 (1982).
Van Camp P. E., et al., PRB34,(1986).,
Christensen N. E. et al., PRB36 (1987). , etc.


## *Single Crystal Diffraction Experiment*

*Large Cylindrical Imaging-Plate Camera @ BL02B1/SPring-8*

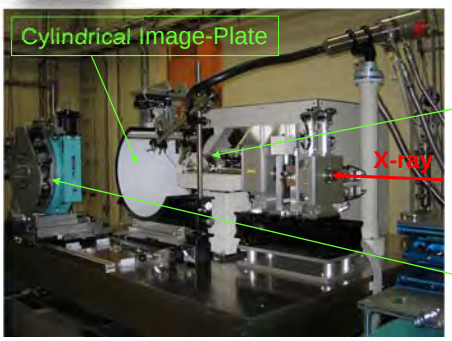


*1/4 χ-goniometer*
- *For data completeness close to 100%.*

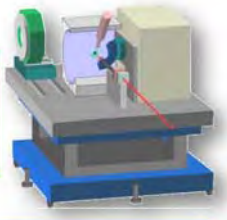

*Single axis goniometer*
- *for cryostat and special sample chamber on phi-axis for in-situ observation*

*Large IP camera and are avertable for a great variety of experiments.*

- *High- and low-temperature experiment*
- *Photo-excited crystal structure*
- *High pressure experiment*

*etc.*

| *Specification:* | |
|---|---|
| *Dynamic range:* | *< $10^6$ counts* |
| *Camera radius:* | *191.3 mm* |
| *Detector area:* | *683(W) x 350(H) mm* |
| *2θ coverage:* | *-60.0 ∼ 144.0°* |

*Extremely high resolution in data collection with high S/N ratio: $DyMnO_3$ data*

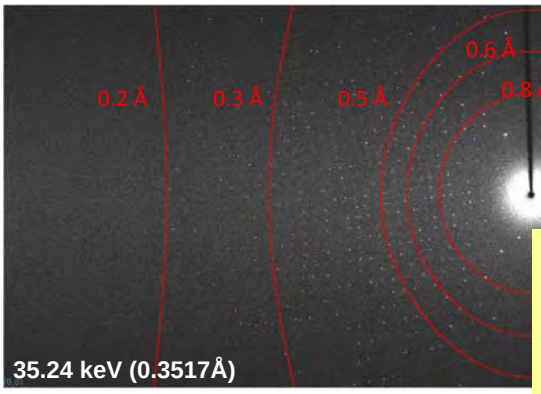


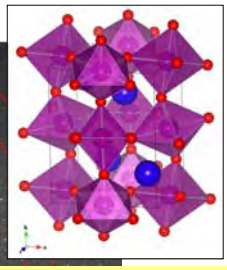

***High resolution data measurement is available for a precise charge density study.***

| $DyMnO_3$ | |
|---|---|
| Crystal size (mm) | 0.03 x 0.03 x 0.03 |
| Cell parameter: | $a$ = 5.82250(10) Å |
| | $b$ = 7.3816(7) Å |
| | $c$ = 5.27400(10) Å |
| | $V$ = 226.67(2) Å$^3$ |
| | $Z$ = 4 |
| Space group | *Pnma* (#62) |
| Wavelength: | 0.3517 Å ( 35.24 keV) |
| Temperature: | 140 K |
| 2$\theta$ max.: | 78.63 ° (0.27 Å) |
| *R*merge: | 4.00 % |
| *R* factor: | 3.13 % (2σ(I)<I) |
| *GOF*: | 1.125 |
| Total measurement time: | 6.5 hours |

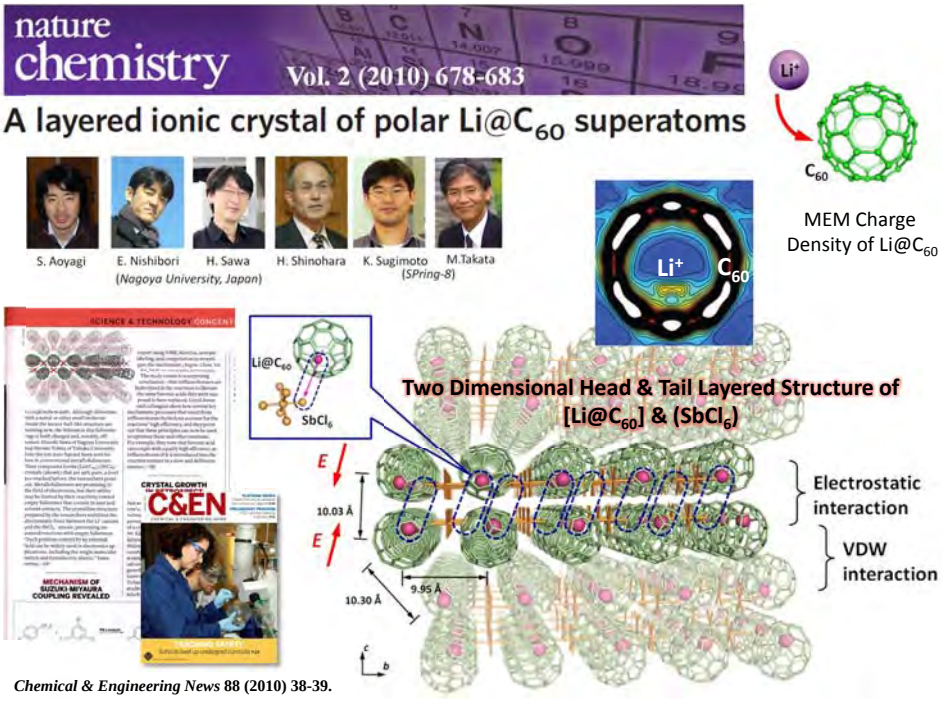


*Chemical & Engineering News* **88 (2010) 38-39.**

## Ultimate Single Crystal Structural Analysis

from 500 nm $BaTiO_3$ single grain powder sample

(Beam size $3.2_W$ x $2.8_H$ um)
$\omega_{total}$=225°, Δω=0.5°, 2θ=30°,
Exposure time 5sec/1 image

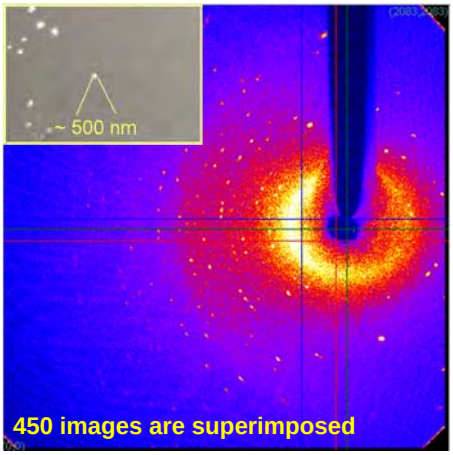


Structure Analysis
by Direct Method

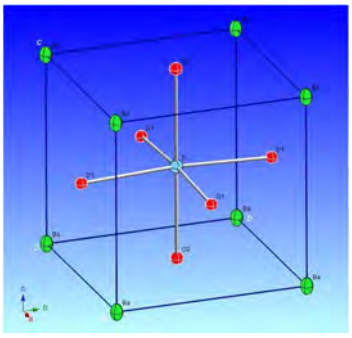

$R_{int}$ 0.0771(4350ref)
$R_1$ 0.0436(2356ref)
$2\theta_{max}$ 65.6°
Completeness 0.925

## *3. Charge Density Refinement by MEM*

***MEM/Rietveld Analysis Application to MOF Chemistry***

***To see mechanism of gas adsorption***

***in nano space***

**$O_2$ in CPL-1**

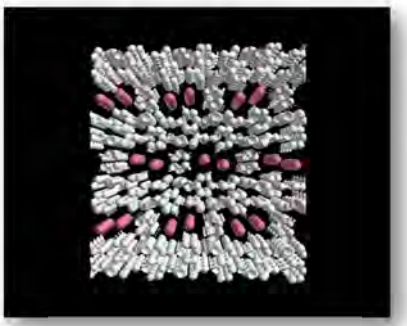

***Science* 298** (2002) 2358

**$C_2H_2$ in CPL-1**

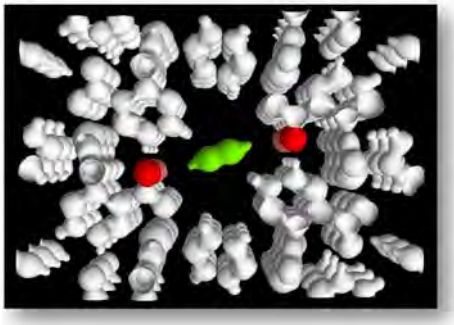

***Nature* 436** (2005) 238

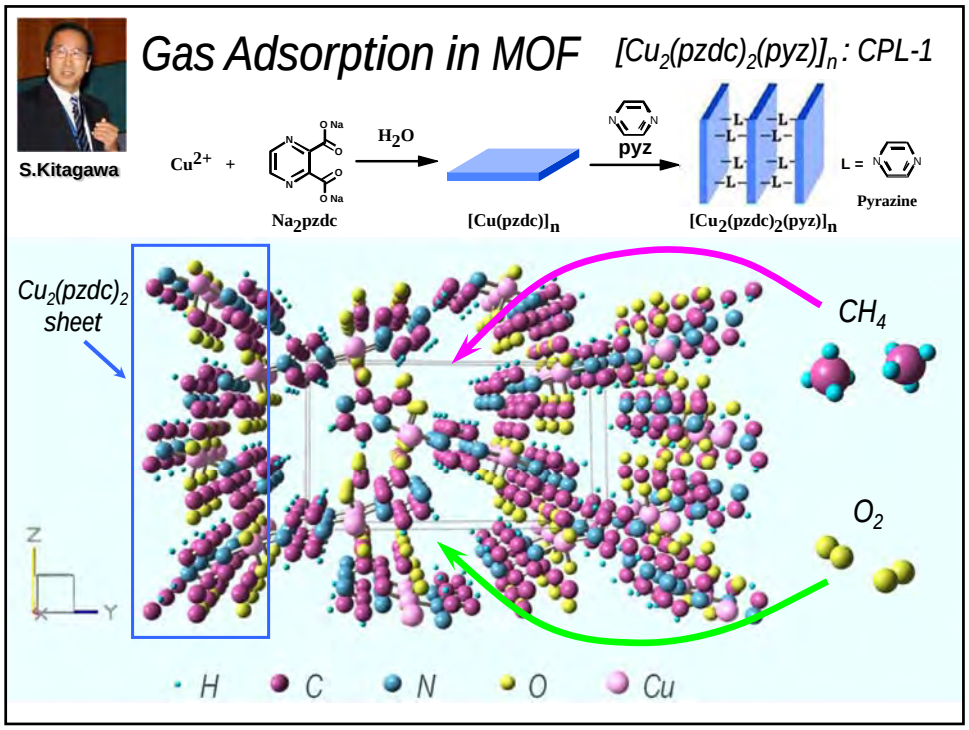
Gas Adsorption in MOF
[Cu2(pzdc)2(pyz)]n : CPL-1
S.Kitagawa
Cu2+ +
H2O
pyz
L =
Pyrazine
Na2pzdc
[Cu(pzdc)]n
[Cu2(pzdc)2(pyz)]n
Cu2(pzdc)2 sheet
CH4
O2
Z
Y
H
C
N
O
Cu

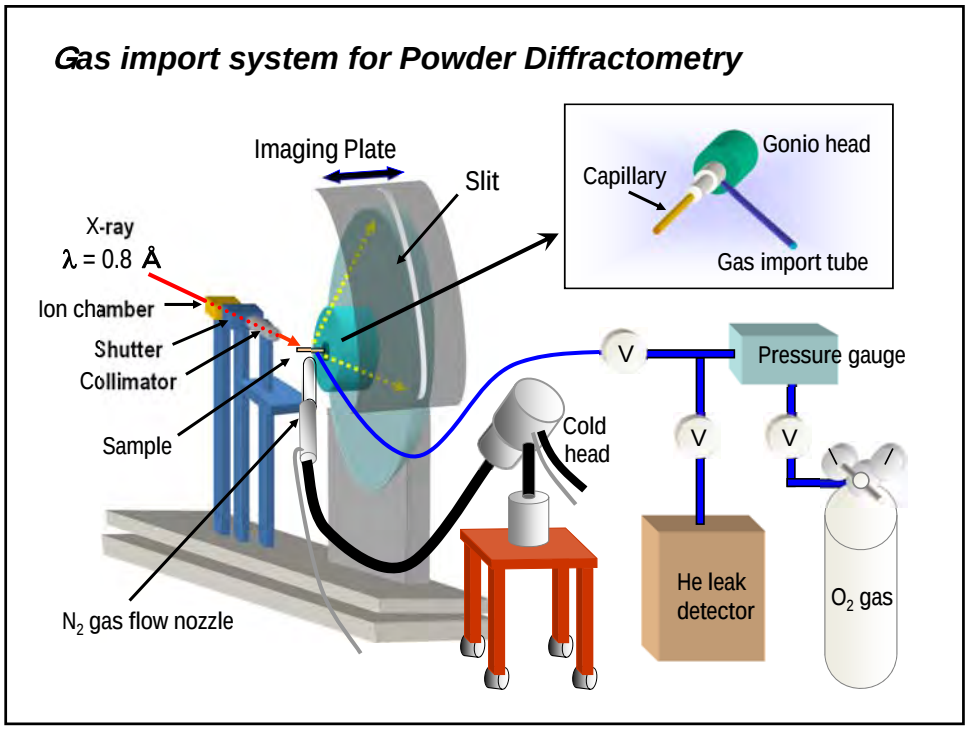
Gas import system for Powder Diffractometry
Imaging Plate
Slit
X-ray
λ = 0.8 Å
Ion chamber
Shutter
Collimator
Sample
N2 gas flow nozzle
Capillary
Gonio head
Gas import tube
Cold head
V
Pressure gauge
He leak detector
O2 gas

*Powder diffraction patterns of $[Cu_2(pzdc)_2(pyz)]_n$ with Oxygen gas adsorption*

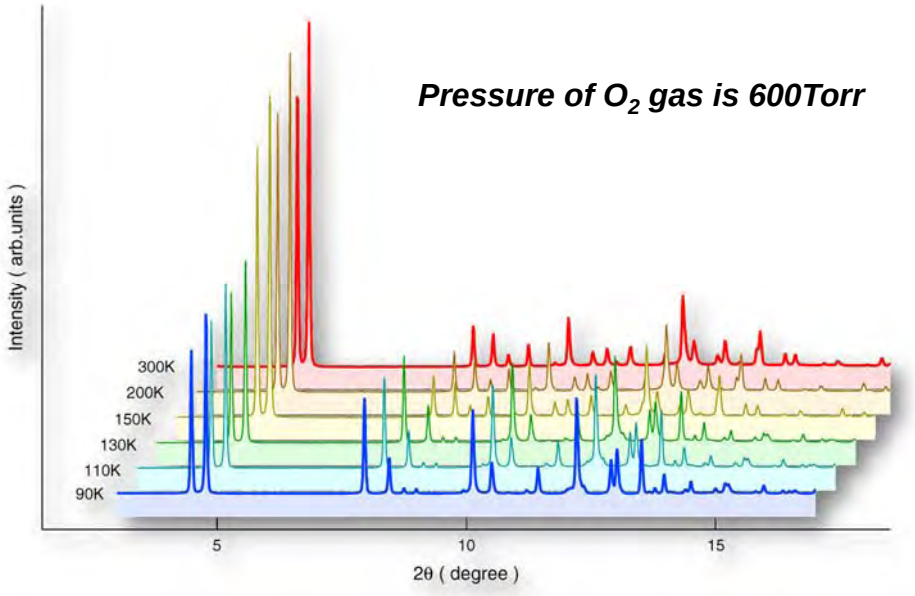


***Pressure of $O_2$ gas is 600Torr***

Structure Model Refinement
by MEM/Rietveld Analysis

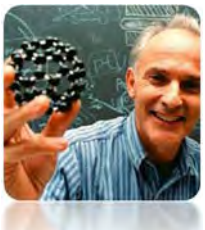

# MEM/Rietveld Analysis

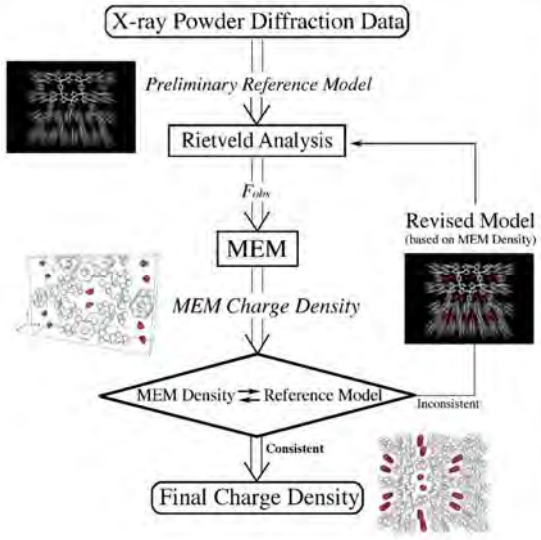


**Preliminary Rietveld Analysis**

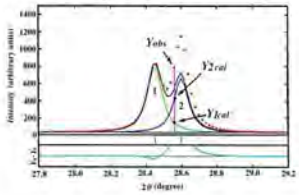

**After the process of**

$$Y_{1obs}(\theta) = Y_{obs}(\theta) \times \frac{Y_{1cal}(\theta)}{Y_{1cal}(\theta) + Y_{2cal}(\theta)}$$

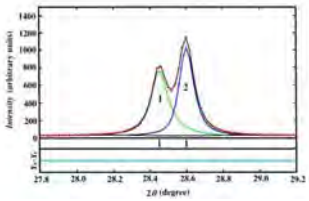

***1st Rietveld fitting based on the initial model***
***$[Cu_2(pzdc)_2(pyz)]_n$ (90K)***

***$R_{WP}$ = 18.5 %  $R_I$ = 54.2 %***

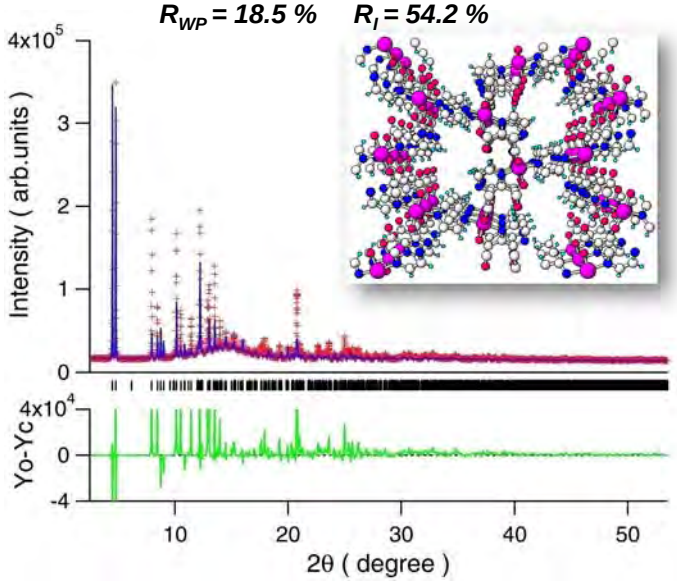

## Model Refinement in MEM/Rietveld Analysis

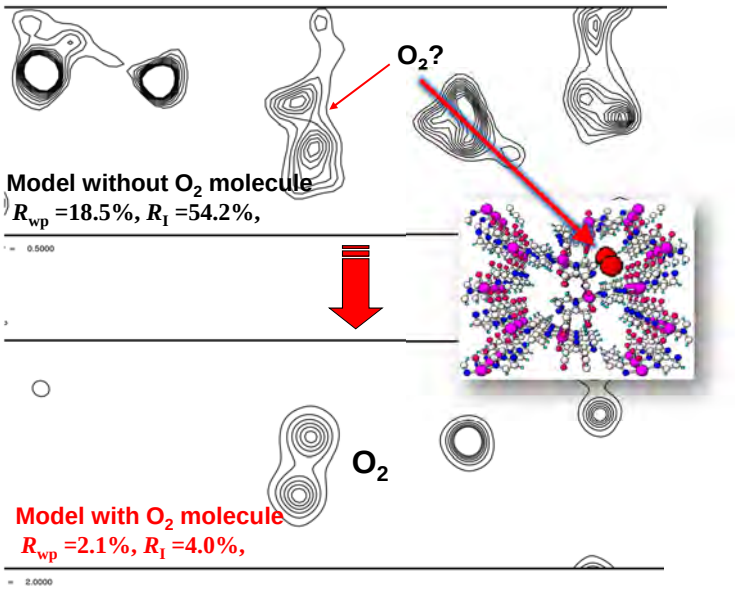


## *Rietveld fitting based on the final model*
## *$[Cu_2(pzdc)_2(pyz)]_n$-$O_2$ (90K)*

**P21/c, Monoclinic:**
**a=4.68759(4)Å, b=20.4373(2) Å, c=10.9484(1) Å, β=96.9479(6)°**

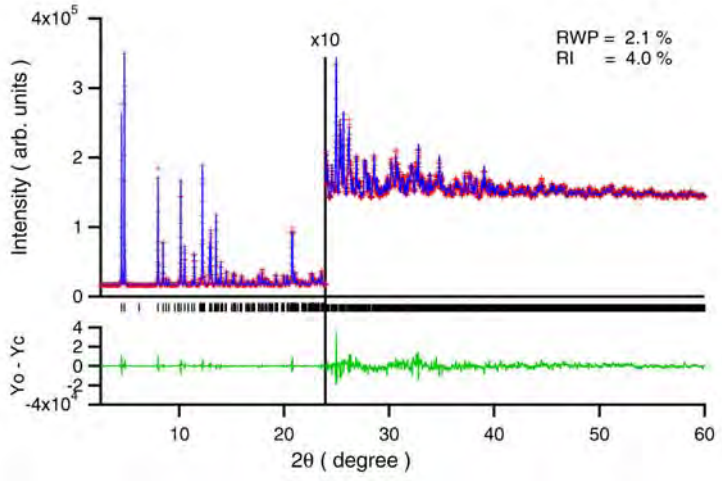

## *Final MEM Charge Density of CPL-1 & CPL-1/$O_2$*

***First Visualization of One Dimensional Array of Physisorbed $O_2$ Molecules in MOF***

Prof. Y.Kubota

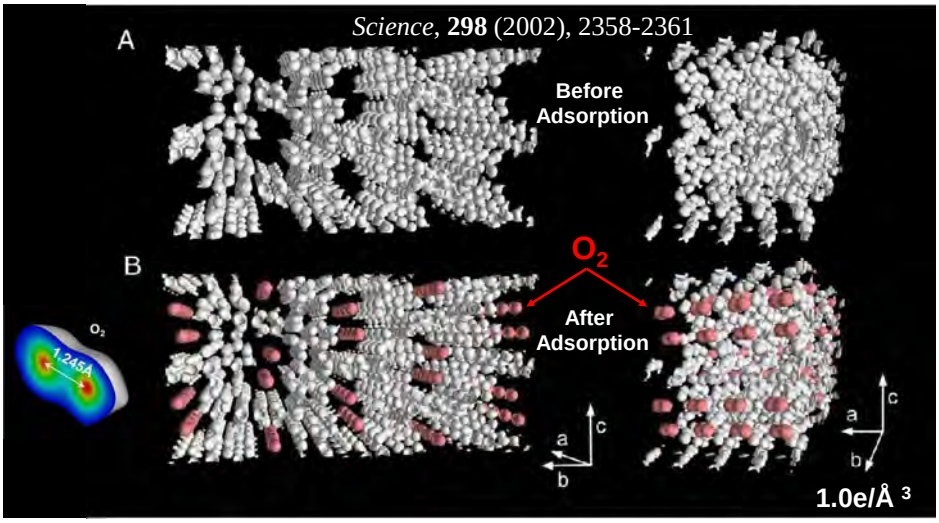


## 1-D Array of $O_2$, $N_2$, $CO_2$, $CH_4$ ,$C_2H_2$ and …

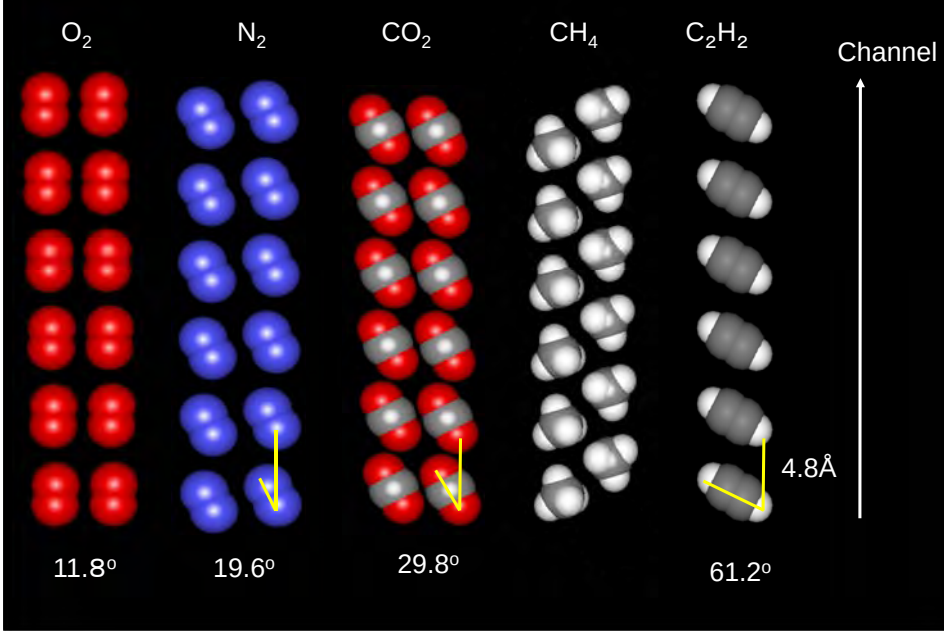

# MEM Charge Density of $C_2H_2$ in CPL-1

***First Visualization of One Dimensional Array of Chemisorbed $O_2$ Molecules in MOF***

***Nature* vol.436 (2005) 238**

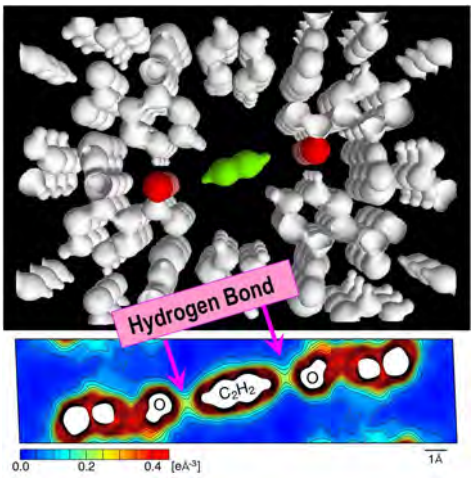


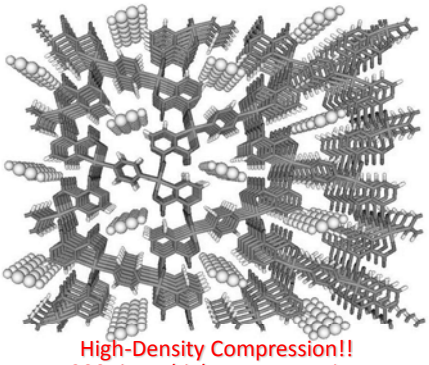

High-Density Compression!!
200 times higher compression
of the lower explosive limit:2 atom. @ R.T.

## Refinement by Omit-Difference MEM Mapping Method

**Prof. E.Nishibori**

Putative Acylphosphatase from *Thermus Thermophilus* HB8

| Statistics of Diffraction Data | |
|---|---|
| Beam Line | BL45XU SPring-8 |
| Space Group | $P2_12_12_1$ |
| Cell Dimensions | $a$ = 29.9 Å, $b$ = 45.7 Å, $c$ = 50.0 Å |
| Resolution | 33.7 – 1.30 Å |
| **Statistics of the Conventional Structural Refinement** | |
| PDB ID | 1ufr |
| $R_{F>4\sigma}$ | 17.85% |
| $R_{free\ (F>4\sigma)}$ | 18.33% |
| Amino Acid Residue | 2 – 88 |
| No. of Waters | 151 |

Disorder of residues, H atoms, and anisotropic thermal displacement are not included in the initial structure model.

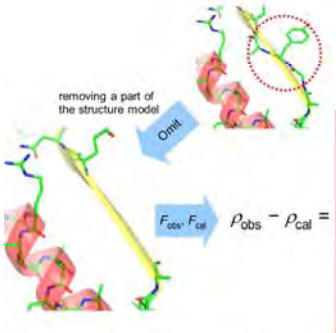


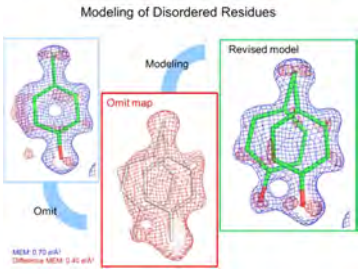


Omitted structure can be reconstructed based on the omit-difference MEM map without model bias.

## Refinement by Omit-Difference MEM Mapping Method

· The reliability factor
  $R_1$ = 17.9 % ⇒ **9.6 %**
· The number of water molecules
  151 ⇒ **203 + 0.6 Cl ion**
· The number of disordered residues
  0 ⇒ **9**
· H atoms
  **93.9 % of total H atoms** were found.

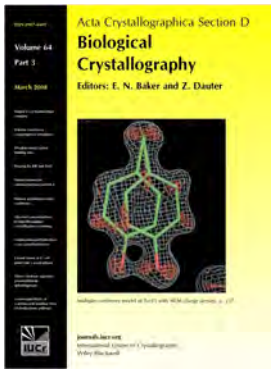


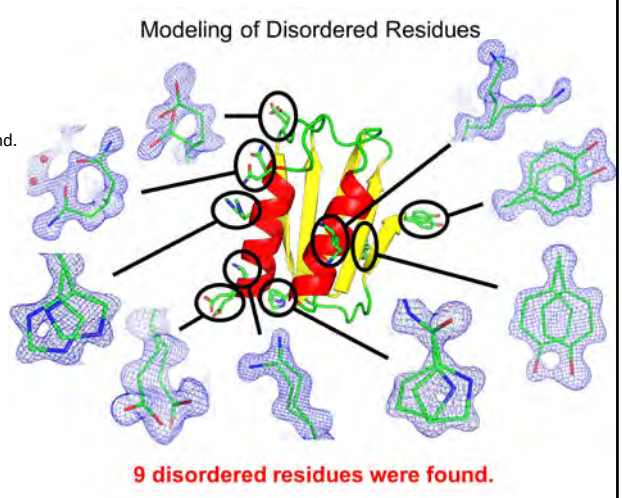


Eiji Nishibori, et al., Acta Cryst. D.(2008)

## 4. Nuclear Density Study by MEM

Fundamental Equation of Neutron Diffraction
to treat negative scattering length

$$F(\mathbf{k}) = V\sum[\rho_+(\mathbf{r})b_+ + \rho_-(\mathbf{r})b_-]\exp(-2\pi i\mathbf{k}\cdot\mathbf{r})$$

Information Entropy Equation of Nuclear Density
based on Neutron Diffraction

$$S(\rho) = S_+ + S_- = \left(-\sum_{k=1}^{N}\rho_k \log\frac{\rho_k}{\tau_k}\right)_+ + \left(-\sum_{k=1}^{N}\rho_k \log\frac{\rho_k}{\tau_k}\right)_-$$

Two MEM equations for Nuclear Density

$$\rho_+ = \exp\left\langle \log\tau_+(\mathbf{r}) + \left(\frac{\lambda}{N}\right)b_+\left[\sum\left[\frac{1}{\sigma^2(\mathbf{k})}\right]\times[F_{cal}(\mathbf{k}) - F_{obs}(\mathbf{k})]\exp(-2\pi i\mathbf{k}\cdot\mathbf{r})\right\rangle\right\rangle$$

$$\rho_- = \exp\left\langle \log\tau_-(\mathbf{r}) + \left(\frac{\lambda}{N}\right)b_-\left[\sum\left[\frac{1}{\sigma^2(\mathbf{k})}\right]\times[F_{cal}(\mathbf{k}) - F_{obs}(\mathbf{k})]\exp(-2\pi i\mathbf{k}\cdot\mathbf{r})\right\rangle\right\rangle$$

*J. Appl. Cryst.* (1993). **26**, 159-165

**Maximum-Entropy-Method Analysis of Neutron Diffraction Data**

BY MAKOTO SAKATA, TATSUYA UNO AND MASAKI TAKATA
*Department of Applied Physics, Nagoya University, Nagoya, Japan*
AND CHRISTOPHER J. HOWARD
*Australian Nuclear Science & Technology Organisation, Lucas Heights, NSW 2234, Australia*
(*Received* 13 *July* 1992; *accepted* 9 *October* 1992)

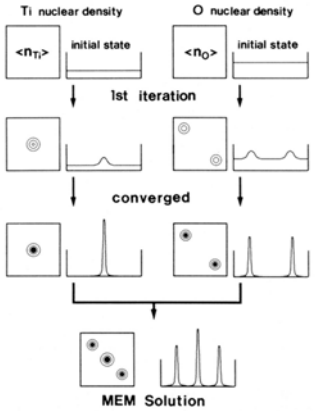


Fig. 1. Third approach: schematic illustration of the iterative procedure used to solve the two MEM equations.

# MEM Nuclear Density of $TiO_2$

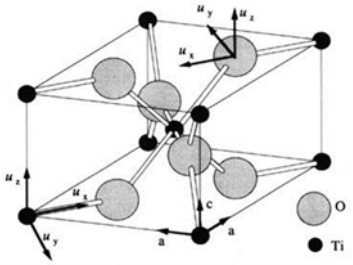


Fig. 1. The rutile structure and the principal axes representing atomic displacements for the Ti and O atoms.

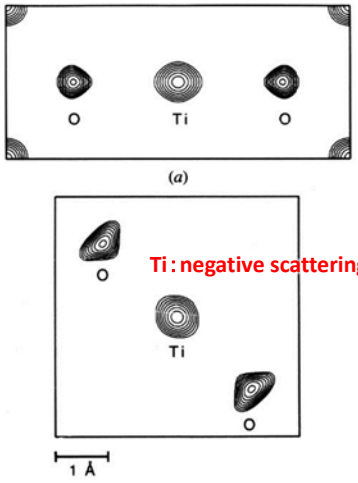


Ti : negative scattering length

Fig. 2. The MEM nuclear density maps of rutile analysed with 128 × 128 × 128 pixels. (*a*) and (*b*) are (110) and (002) planes, respectively. The contour lines are on a logarithmic scale at $0.01 \times 5^n$ ($n = 0, 1, ..., 8$) ($N$ Å$^{-3}$).

## Complementary Information of Bonding Nature in Nuclear Density

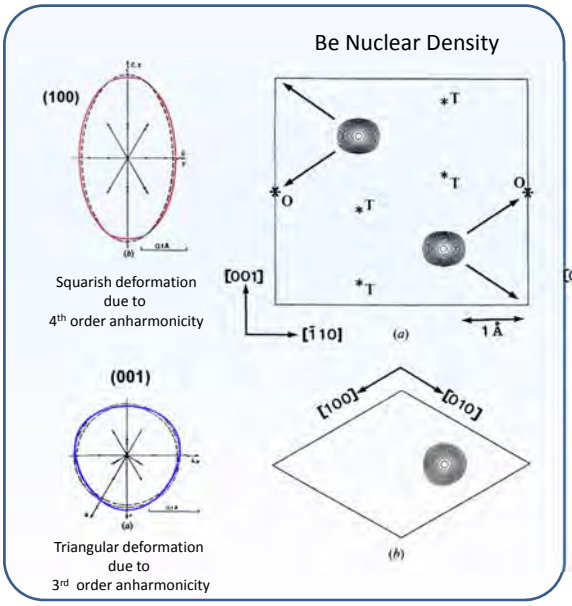

# 5. Application

Direct Observation of
Orbital & Charge Order in Manganite
by MEM/Rietveld Method

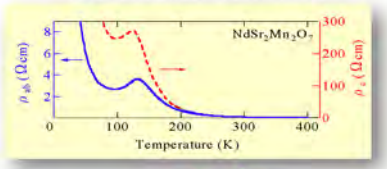


Orbital Order Model

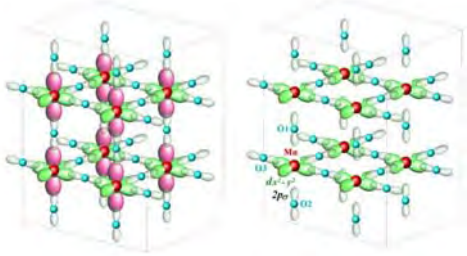

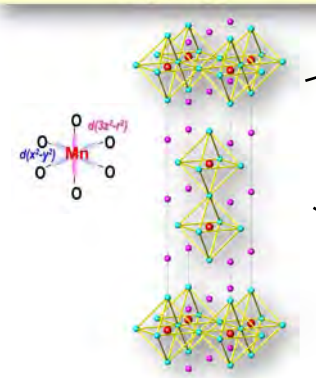


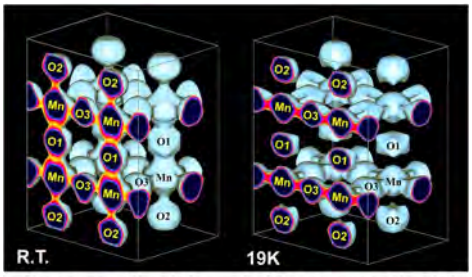


*Paramagnetic state* *Anti-ferromagnetic state*

The MEM Charge Densities of $NdSr_2Mn_2O_7$

M.Takata *et al. JPSJ Lett.* 68(1999)2190

## *Finding Variety of Orbital/Charge Order in Manganite*

Dr. K.Kato

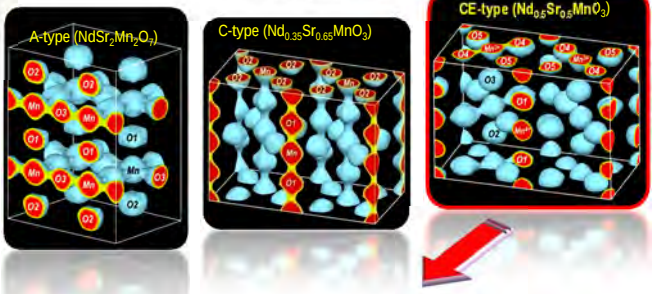


Prof. Y.Moritomo

Charge Order visualized in MEM Electrostatic Potential

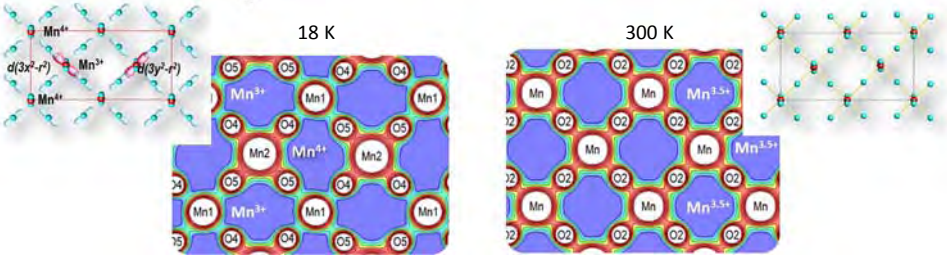


Electrostatic potential on 0.8 $e$/Å$^3$ iso-surface

K. Kato et al., *Phys. Rev. B* 77, 081101(R) (2008).

## Nuclear Density of KDP ($KH_2PO_4$)

investigation of hydrogen bond

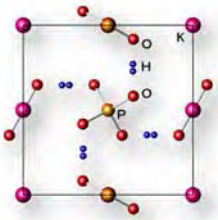


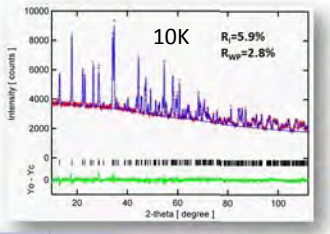


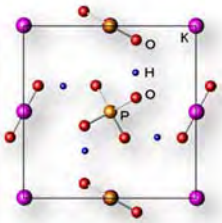


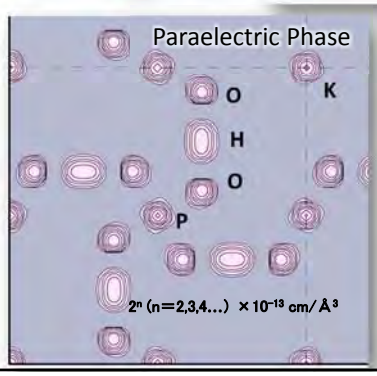


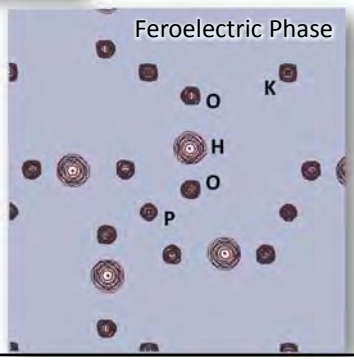


*MEM can just visualize the information included in data.*

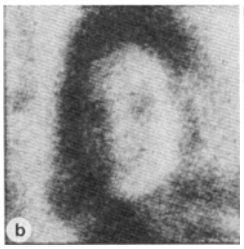


**Poor Counting Statistics**


**MEM Susie Based on (b)**


Susie (original)


**Better Counting Statistics**


**MEM Susie Based on (d)**